Lehigh University
Lehigh Preserve

Theses and Dissertations

1988

Heat transfer in boron nitride filled epoxy composites /

Keith A. Brown
Lehigh University

Follow this and additional works at: https://preserve.lehigh.edu/etd

Part of the Manufacturing Commons

Recommended Citation
Brown, Keith A., "Heat transfer in boron nitride filled epoxy composites /" (1988). *Theses and Dissertations*. 4832.
https://preserve.lehigh.edu/etd/4832

This Thesis is brought to you for free and open access by Lehigh Preserve. It has been accepted for inclusion in Theses and Dissertations by an authorized administrator of Lehigh Preserve. For more information, please contact preserve@lehigh.edu.

Heat Transfer in Boron Nitride Filled Epoxy Composites

by

Keith A. Brown

A Thesis
Presented to the Graduate Committee
of Lehigh University
in Candidacy for
the Degree of
Master of Science
in
Manufacturing Systems Engineering

Lehigh University
1987

Certificate of Approval

This thesis is accepted and approved in partial fulfillment of the requirements for the degree of Master of Science.

11/4/1987

Date

Walter Charles Hahn, Jr.

Professor in Charge

Director of MSE Program

Stephen K. Tarby

Acting Chairman of Materials Sci. and Eng. Dept.

Acknowledgements

My parents deserve highest recognition for helping me to succeed in my endeavors. I was not easy on them and I love and thank them for all they have done for me. I'm sure they didn't know what to expect from me when it seemed as if I wasn't even going to complete high school, but they stuck in there, giving me support in their quiet, subtle way which makes it so valuable. Thanks again.

My thesis advisor, Dr. Hahn, is not just the guy who (hopefully) will sign this paper; he is also a generous friend and super professor. He sparked my interest in materials so much that I transferred into materials engineering. It was fun to learn from Dr. Hahn. He was quick to point out that learning the periodic table was easier when he was a student (you see there were only four elements then...fire, earth, air, and water). And who could forget how he called on us to demonstrate our vast (or "half-vast") knowledge of chemistry? Thanks for doing everything your way...the right way.

I am indebted to Andrea Braun, a coop student studying Metallurgical Engineering at Purdue University, for her contributions to this project. Andrea performed most of the experimental work presented in this paper and was very helpful while I was on leave of absence.

My manager, George Galyon, deserves recognition for his part in this work. George has been very supportive of my work; encouraging me to devote part of my time at IBM to my thesis and granting me an educational leave of absence. I thank the IBM Corporation for its commitment to personal development which made this work possible.

I would also like to thank all of the great people in Department C30 at

IBM who have helped me out over the past couple of years by sharing their knowledge with me and helping to shape me professionally.

Thanks to Jeff Eid and Vince Antonetti at IBM for their advice with this project and also for the use of the Advanced Thermal Laboratory.

I am grateful to the Alumni Association of Lehigh University for its fellowship support of my graduate work.

Table of Contents

ABSTRACT 1

1. INTRODUCTION 3

2. SPECIMEN PREPARATION 6

2.1 Chemicals used and suppliers 6

2.1.1 Boron nitride 6

2.1.2 Epoxy resin 7

2.1.3 Coupling agent 8

2.1.4 Curing agent 8

2.1.5 Epoxy diluent 9

2.1.6 Antifoam compound 10

2.1.7 Epoxy stripper 10

2.1.8 Components used in each specimen 10

2.2 Procedures used to prepare specimens 11

2.2.1 Degas resin 11

2.2.2 Measure components 12

2.2.3 Blend components 12

2.2.4 Casting the specimen 13

2.2.5 Curing the specimen 14

2.2.6 Machining operations 14

2.2.7 Final inspection 14

3. TESTING PROCEDURES 16

3.1 Hardware Preparation 16

3.2 Software preparation 21

3.3 Making a test run 22

4. RESULTS AND DISCUSSION 23

4.1 Retention of dimensions 24

4.2 Thermal Conductivity Results 26

4.3 Evaluation of heat losses 28

4.4 Specimen mass and density 30

4.5 Comparison to Previous Work 30

4.6 Suggestions for Future Work 32

5. Models of Thermal Conductivity of Composite Systems 34

5.1 Classical Models 35

5.1.1 Rule of Mixtures 36

5.1.1.1 Equation used to model system 36

5.1.1.2 Performance of the model 36

5.1.2 Inverse rule of mixtures 36

5.1.2.1 Equation used to model system 36

5.1.2.2 Performance of the model 36

5.1.3 Geometric Mean Model 37

5.1.3.1 Equation used to model system 37

5.1.3.2 Performance of the model 37

5.2 Newer Models 37

5.2.1 Maxwell Theoretical Model 37
5.2.1.1 Equation used to model system 37
5.2.1.2 Performance of the model 38
5.2.2 Bruggeman Theoretical Model 38
5.2.2.1 Equation used to model system 38
5.2.2.2 Performance of the model 38
5.2.3 Lewis and Nielsen Semi-Theoretical Model 38
5.2.3.1 Equation used to model system 39
5.2.3.2 Performance of the model 39
5.2.4 Cheng and Vachon Theoretical Model 39
5.2.4.1 Equation used to model system 39
5.2.4.2 Performance of the model 40
5.2.5 Agari and Uno Theoretical Model 40
5.2.5.1 Equation used to model system 40
5.2.5.2 Performance of the model 41
5.2.6 Hamilton and Crosser Semi-Theoretical Model 41
5.2.6.1 Equation used to model system 41
5.2.6.2 Performance of the model 41
5.3 Summary of Models 42
6. CONCLUSIONS **43**
Appendix A. Description of test apparatus **44**
Appendix B. Equipment used in this project **46**
B.1 Specimen preparation and inspection 46
B.2 Test Apparatus 47
Appendix C. Data **50**
Appendix D. Data from Previous Work **57**
Appendix E. Results of Other Models **58**
Appendix F. Description of Thermal Comparator **60**
REFERENCES **62**
VITA **66**

List of Figures

Figure 2-1:	Sketch of epoxy test specimen	15
Figure 3-1:	Schematic of thermal conductivity test apparatus	17
Figure 3-2:	Photograph of thermal conductivity test area	18
Figure 3-3:	Schematic of test column	19
Figure 3-4:	Photograph of test column	20
Figure 4-1:	Photograph of test specimens	23
Figure 4-2:	Photograph of specimen #95	24
Figure 4-3:	Photograph of specimen # 52	25
Figure 4-4:	Thermal Conductivity vs. Loading of Boron Nitride	29
Figure 4-5:	Specimen Density vs. Loading of Boron Nitride	31

List of Tables

Table 2-1:	Components used in each specimen	11
Table C-1:	Specimen Thickness	50
Table C-2:	Calculations of Thermal Conductivity	51
Table C-3:	Thermal Conductivity versus Boron Nitride Loading	52
Table C-4:	Experimental vs. Predicted Thermal Conductivity	53
Table C-5:	Heat Losses in Trial Runs of Specimen #52	54
Table C-6:	Heat Losses and Vacuum Pressure	54
Table C-7:	Specimen Mass and Density	55
Table C-8:	Boron Nitride Volume and Weight Percent	56
Table D-1:	Thermal Conductivity Data of R. M. Smith	57
Table E-1:	Experimental Thermal Conductivity Compared to Series, Parallel, and Geometric Mean Models	58
Table E-2:	Experimental Thermal Conductivity Compared to Models by Maxwell, Bruggeman, and Cheng and Vachon	59

ABSTRACT

This thesis project is concerned with the development of a thermally conductive, electrically insulating epoxy composite. Boron nitride powders were used to enhance the thermal conductivity of bisphenol-A epichlorohydrin epoxy resins. The powders were supplied by Union Carbide under the product names HCM and HCP, HCP being the finer of the two. Cylindrical test specimens were prepared with different concentrations of boron nitride.

The thermal conductivity of each specimen was then determined. Heat was conducted through a series of cylinders; one aluminum, one Armco iron, and one epoxy. The heat flux in the epoxy specimen was conservatively estimated to be equal to that in the Armco iron cylinder. Fourier's equation for heat conduction was used to calculate the thermal conductivity of the epoxy specimen. As expected, the thermal conductivity was strongly related to the loading of boron nitride. A number of models of thermal conductivity of composites were considered, however, due either to deficiencies in the models or to the irregular shape and size of the boron nitride powders, none of these models well represented the boron nitride epoxy system. As a consequence, the following empirical model was developed:

$$\lambda = 0.22 + 0.021\text{wt\%HCM} + 0.027\text{wt\%HCP} + 0.81\times10^{-6}(\text{wt\%HCP}+\text{wt\%HCM})^{3.6} + 0.013(\text{wt\%HCM}\times\text{wt\%HCP})^{0.6}$$

where:

λ = thermal conductivity of epoxy composite, $\frac{watts}{m\ ^oK}$

wt% HC(M,P) = weight percent HC(M,P) boron nitride in the specimen.

This equation fits the data with a correlation coefficient of 0.98.

It was determined that the losses, calculated as the difference between the heat flux generated by the heater and the heat flux passing thru the Armco iron cylinder, were minimized when testing was performed in a vacuum.

This test method produced consistent data which is also believed to be fairly accurate. However, a major drawback of this method is the time required to perform a test; a thermal comparator operates much more quickly.

Chapter 1
INTRODUCTION

Epoxy-based composite materials have been attractive for a number of years due to their generally excellent resistance to both elevated temperatures and chemical attack. Epoxy composites derive their properties from the basic chemistry of the epoxy as well as from fillers. Fillers are used to improve some characteristic of the epoxy system, such as cost, or electrical or thermal conductivity. The loading, or concentration[1] determines the degree to which material properties are enhanced by the filler. For example, if it is desired to improve the thermal conductivity of a composite material by adding a thermally conductive filler, then the higher the loading, the higher the thermal conductivity of the composite. Because the loading will influence a number of material properties, including the ability of the composite to withstand thermal shock, it is incorrect to assume that the composite is most desirable when the loading is a maximum.

Epoxies are used in electronic applications to bond a heat generating device, such as an integrated circuit, to a heat absorbing device, such as an aluminum heat sink. The operating temperature of the device is determined by a number of factors; including the power consumption, the interfacial resistances, the flow of air, and the thermal conductivity of the epoxy composite.

Epoxy composites which are both thermally and electrically conductive often use silver as a filler[1]. Alumina powder is frequently used as a filler for thermally conductive, electrically insulating epoxy composites[2]. Alumina is an

---

[1]Throughout this paper, the concentration of filler in the composite will be reported in units of weight percent.

electrical insulator, has good thermal conductivity, and is inexpensive. Laboratory grade alumina powder costs[3] only about $20/kg, and most alumina-filled epoxy composites use alumina which costs even less than this. Economics are responsible for the continued heavy use of alumina-filled epoxies.

The work discussed in this manuscript was concerned with the development of an epoxy composite that is both thermally conductive and electrically insulating. Boron nitride powders were used as filler in this work. Boron nitride is not a new material, but has not found widespread use due to its cost; high purity boron nitride powders can cost[4] as much as $275/kg. Why, then should one bother to even look at boron nitride as a filler? A most attractive property of boron nitride is its superior thermal conductivity. Boron nitride has a thermal conductivity[5] of 41.5 W/m °K while alumina has a thermal conductivity[6] of 30.1 watts/m °K. This may not seem like a dramatic difference, but in many electronics applications, even a small decrease in operating temperature can have a significant impact on reliability[7].

This work is also concerned with a method for testing epoxy composites to determine their thermal conductivity. A thermal comparator is often used for this purpose. This approach was not used in this work. The method used in the work presented here makes use of Fourier's equation for heat conduction:

$$Q = \frac{-\lambda \Delta T}{\Delta X}$$

where:

Q = heat flux, $\frac{watts}{m^2}$

λ = thermal conductivity of epoxy composite, $\frac{watts}{m\,^oK}$

$\frac{\Delta T}{\Delta X}$ = temperature gradient, $\frac{^oK}{m}$

The apparatus consisted of a column with a heater at the top and a cold plate at the bottom. Heat flowed down from the heater, through an aluminum cylinder, through a test specimen, through an Armco iron cylinder and finally reached the cold plate. Thermocouples placed along the column were used to determine the thermal gradients in each specimen. The heat flux was calculated based on the temperature gradient in the iron cylinder, as its thermal conductivity was well known. The thermal conductivity of the epoxy specimen was calculated by substituting the heat flux and temperature gradient into Fourier's equation. A more detailed description of the test apparatus appears elsewhere in this manuscript.

Chapter 2
SPECIMEN PREPARATION

2.1 Chemicals used and suppliers

2.1.1 Boron nitride

The boron nitride powders used in this work were supplied by the Electronics Division of the Union Carbide Corporation. These powders differ primarily in particle size; HCM is composed of larger particles than HCP. Union Carbide furnished the typical properties which are listed below[8, 9, 10].

Property	Type of boron nitride	
	cat. #H-3205 HCM	cat. #H-3250 HCP
Density, $\frac{g}{cm^3}$	2.26	2.26
Tap density, $\frac{g}{cm^3}$	0.80	0.20
Chemical analysis, %		
Boron and nitrogen	99+	99+
Maximum oxygen	0.5	0.5
Maximum carbon	0.2	0.3
Maximum other metallic impurities	0.1	0.1
Surface area, $\frac{m^2}{g}$	4	15
Screen analysis	0% on 48 mesh, 90% minimum thru 48 on 200 mesh	94.5% minimum thru 325 mesh
Particle Size Distribution, μm		
range:	100 - 300	1.5 - 20
median:	175	8

These two forms were chosen because of their high purity. The two particle size distributions are desirable as they permit a blend to be made in which the finer particles occupy the interstices formed by the coarser particles. It was expected that this would result in increased thermal conductivity due to increased particle-particle contact. It was difficult to achieve high loading levels when HCP boron nitride was used alone because the finer particles presented an increased surface area which had to be wet.

2.1.2 Epoxy resin

Three conventions will be followed for the remainder of this chapter; all properties referred to are those present at 25°C, density is reported in units of g/cm^3 and viscosity is reported in units of Pa·s (kg/m·s).

The first resin used, Epon 828, was supplied by the Shell Chemical Company[11, 12, 13]. Epon is the industry standard for a resin composed of the diglycidyl ether of bisphenol-A. While the performance properties of this resin are no longer state of the art, its long history has produced an abundance of available technical information. This resin is also flexible in the sense that it can be cured by a number of different curing agents and curing schedules. This resin has a density of 1.17.

Another resin which was used, DER 332, was supplied by the Dow Chemical Company[14, 15, 16]. This resin has a density of 1.16. Like Epon, this resin is the diglycidyl ether of bisphenol-A, however, the Dow resin has a lower viscosity. Epon 828 has a viscosity of 11.0-15.0 while DER 332 has a viscosity of 4.0-6.0. The low viscosity is due to its high purity and lack of chemical fractions. Low viscosity is desirable because of improved blending. DER 332

was adopted for use part of the way thru the project because its reduced viscosity facilitated producing heavily loaded specimens.

2.1.3 Coupling agent

A coupling agent, 3-glycidoxylpropyl-trimethoxysilane, was supplied by the Dow Corning Corporation under the product name Z-6040[17, 18]. The density of this coupling agent is 1.07. This coupling agent has the epoxy reactivity which permits it to be intimately associated with the epoxy resin. The coupling agent also has trimethoxysilyl reactivity and therefore can bond to inorganic surfaces. For this work, the inorganic surfaces of interest were the boron nitride particles. The silane may be added directly to the resin or used as a surface pretreatment where the particles are soaked with the silane, or a dilute aqueous solution of the silane, and then dried prior to adding the particles to the resin. In the latter method, it is difficult to determine how much silane is, or should be, used. Dow recommends using the silane at a concentration of 0.5-2.0 phr, where phr stands for parts (by weight) per one hundred parts resin.

2.1.4 Curing agent

One curing agent which was used, Epon Curing Agent Z, was supplied by the Shell Chemical Company[19]. Curing Agent Z is a liquid aromatic amine eutectic with a viscosity of approximately 2 and a density of 1.20. This curing agent functions over a wide range of temperatures, from 65°C to 200°C. If desired, the resin may be cured by a two step process; in the first the resin becomes partially crosslinked. Because this "B-stage" material is partially crosslinked, it is rigid enough to be handled. Curing may be completed by

exposing the "B-stage" resin to elevated temperatures. For most applications, the optimum concentration of Curing Agent Z is 20 phr.

Another curing agent which was used, 2-Ethyl-4-Methylimidazole, was supplied by Air Products and Chemicals, Inc., under the name IMICURE EMI-24[20]. EMI-24 functions over a wide range of curing temperatures, between 60 and 177 degrees Celsius. This curing agent has a viscosity of 4-8 and a density of 0.985. In use, the main difference between EMI-24 and Epon Curing Agent Z is that one uses much lower concentrations of EMI-24, usually only 4 phr.

2.1.5 Epoxy diluent

An epoxy diluent, the diglycidyl ether of neopentyl glycol, was supplied by Wilmington Chemical Corporation under the product name Heloxy WC-68[21]. Its density is 1.05. A diluent reduces the viscosity of the epoxy system to permit easier blending and more effective removal of entrapped gasses. Shell[22] reports that adding 13 weight percent diglycidyl ether of neopentyl glycol to Epon 828 reduces the resin's viscosity from approximately 11.0 to approximately 2.0. While the supplier does not indicate recommended concentrations, it should be noted that using too much diluent will impair curing and cause the specimen to be tacky. A tacky specimen cannot be properly machined and/or will not retain its dimensions during testing.

2.1.6 Antifoam compound

An antifoam compound was supplied by the Dow Corning Corporation under the name DB-100[23]. DB-100 is a compounded silicone fluid of density 1.00. The antifoam compound may be added to the epoxy system directly or may be predispersed into one of many solvents. Adding the antifoam compound to a solvent permits more accurate measurement as the compound is used at concentrations in the range of 10 to 200 ppm, where one drop more or less can make quite a difference. In this work, methyl ethyl ketone was used as a solvent.

2.1.7 Epoxy stripper

An epoxy stripper, MS-115, was supplied by the Miller-Stephenson Chemical Company[24]. This stripper was used for cleaning any equipment which came in contact with the uncured resin.

2.1.8 Components used in each specimen

Table 2-1 indicates which of the components just discussed were used in preparing each specimen.

Component	Specimen Number							
	0	52	57	61	62	63	64	65
Epon 828 resin	X	X	X	X	X	X		X
DER 332 resin							X	
Z-6040 silane		X	X	X	X	X	X	X
Curing agent Z		X	X	X	X	X	X	X
Heloxy WC-68		X		X	X	X	X	X
HCM boron nitride			X	X	X	X	X	X
HCP boron nitride		X	X	X	X	X	X	X

	68	70	73	74	75	94	95	102
DER 332 resin	X	X	X	X	X	X	X	X
Z-6040 silane	X	X	X	X	X	X	X	X
Curing agent Z	X	X	X	X	X			
IMICURE EMI-24						X	X	X
Heloxy WC-68	X	X	X	X	X	X		X
HCM boron nitride	X	X	X	X	X	X		X
HCP boron nitride							X	X
DB-100 antifoam						X	X	X

Table 2-1: Components used in each specimen

2.2 Procedures used to prepare specimens

2.2.1 Degas resin

The resins used were found to contain significant amounts of dissolved gasses which, if not extracted, produced porosity in the casting. It was determined that the porosity could be reduced by degassing the resin prior to the addition of any other components. Degassing was accomplished by placing

the resin in a vacuum oven at 70°C for approximately twenty minutes. A mechanical pump produced a vacuum of 740 to 760 mm mercury. While under the vacuum, gasses were observed escaping from the resin as bubbles came to the surface and broke.

2.2.2 Measure components

In measuring the components, several goals had to be accomplished simultaneously: 1) measure the correct amounts of diluent, silane, curing agent, and antifoam compound with respect to the amount of resin to be used, 2) measure the correct amounts of resin and boron nitride powder to produce the desired loading level, and 3) assure that the batch was large enough to produce a sufficiently large casting. This last consideration was designed to compensate for the losses due to mixing and casting.

2.2.3 Blend components

The components were combined in the following steps:

1. The boron nitride powder(s) were placed into a 50 ml polypropylene beaker. It was necessary to use a beaker this size to prevent splashing during the blending process. Polypropylene was selected because it did not react with the epoxy and because it was not susceptible to damage due to the blades of the blending equipment.

2. The silane was added to the boron nitride powder(s) and mixed for thirty seconds using the "Dispersator" mechanical blending apparatus.

3. The epoxy resin, diluent (if any) and antifoam compound (if any) were added to the beaker. The mixture was stirred with a wooden stirrer until it appeared homogeneous and then blended for thirty seconds using the dispersator.

4. The dispersator did quite a good job of blending the components, but it also added air to the mixture. The mixture was degassed to remove as much of this air as possible. The beaker was placed in a 70°C vacuum oven. As the vacuum increased, bubbles would form, rise to the surface, and (usually) rupture. If the mixture foamed, the vacuum oven was alternately evacuated and vented to encourage the bubbles to rupture. The beaker was removed from the vacuum oven after a total of fifteen minutes.

5. In the final step, the curing agent was blended into the mixture using a wooden stirrer.

2.2.4 Casting the specimen

The mixture was poured into a 28.58 mm diameter plastic mold. A Caplug[25] specimen cup was used as the mold.

2.2.5 Curing the specimen

The casting was placed in a 60°C atmospheric oven. After one hour, the oven temperature was increased to 70°C. After two hours at 70°C, the casting was removed from the mold and postcured for one hour at 100°C. After postcuring, the specimen was examined. Specimens containing large bubbles were rejected.

2.2.6 Machining operations

A diamond saw was used to remove the top and bottom portions of the cylinder and reduce it to a thickness of approximately 10 mm. After the cutting operation, the ends of the cylinder were ground flat and parallel to a thickness of 9.53 mm. Three 0.57 mm diameter thermocouple holes were drilled to a depth of 7.62 mm. These dimensions are illustrated in Figure 2-1.

2.2.7 Final inspection

The specimen was carefully examined for defects. Excessive porosity or out of tolerance dimensions were the most common grounds for rejection. Due to the very small diameter drill bit which was used, several bits broke off in the specimens. These specimens were rejected. Ten of the twenty-five specimens reaching final inspection were rejected.

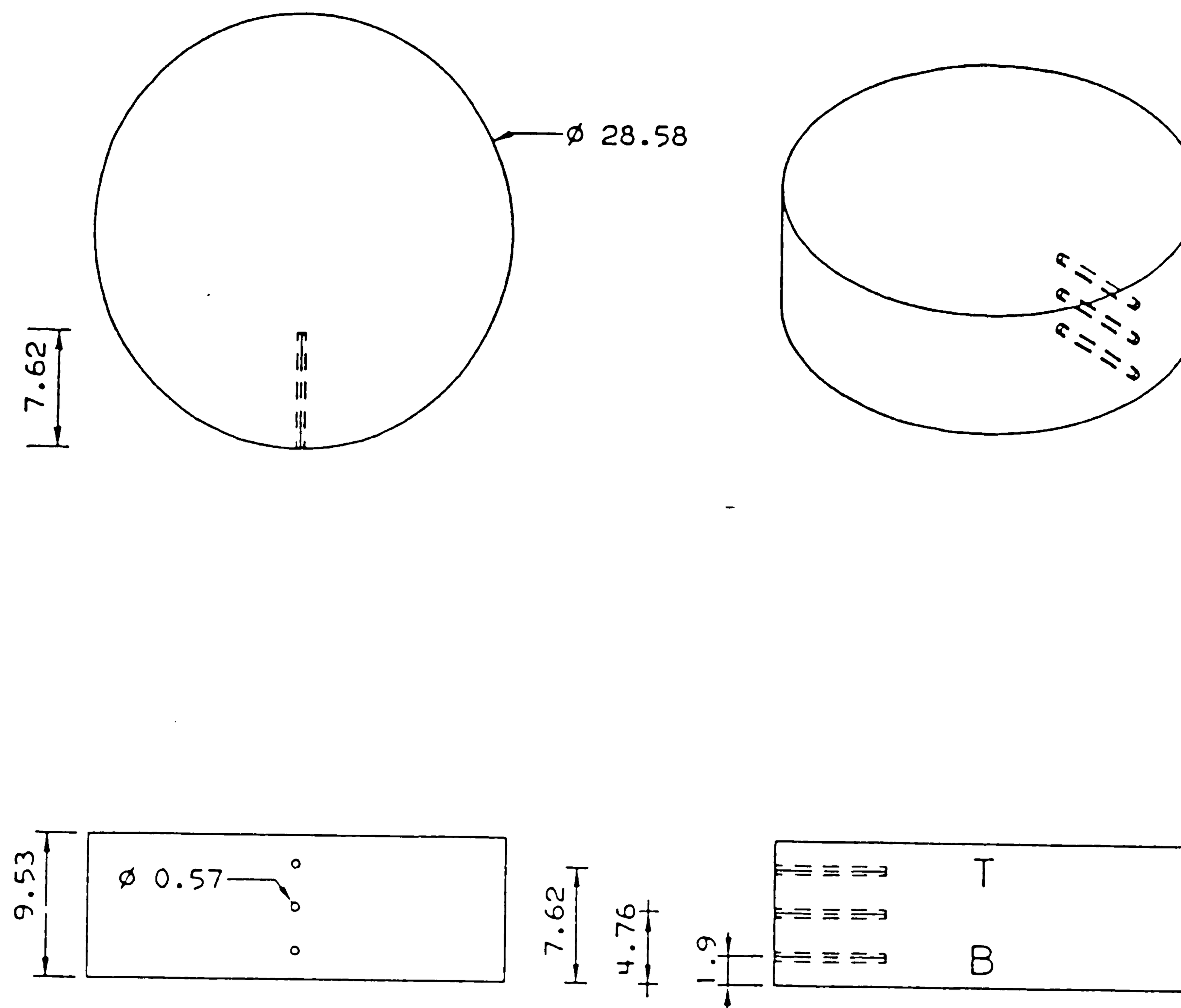

Figure 2-1: Sketch of epoxy test specimen

Chapter 3
TESTING PROCEDURES

This chapter describes how the test rig was operated. Testing involved essentially three stages; the first was concerned with preparing the test rig, the second stage involved running a computer program, and the third was concerned with actually making the test run. Figure 3-1 is a schematic of the thermal conductivity test apparatus. Figure 3-2 is a wide angle view of the test apparatus and supporting hardware.

3.1 Hardware Preparation

The load cell power and on/off limit controller were activated. The on/off limit controller was set to the maximum desirable test temperature. The valve on the compressed air tank was opened.

A small amount of Dow Corning 340 silicone heat sink compound was applied to the tips of four bare, 0.13 mm diameter, 910 mm long copper-constantan thermocouples. The thermocouple tips were inserted into the holes in the aluminum cylinder which are referred to as one through four in Figure 3-3. After the thermocouples were fully inserted into the appropriate holes, the wires were wrapped around the cylinder once and secured with tape.

A thin, uniform layer of heat sink compound was applied to both ends of the aluminum cylinder and both ends of the epoxy specimen. This step was intended to reduce the interfacial resistances between the heater and the aluminum cylinder, the aluminum cylinder and the epoxy cylinder and the epoxy cylinder and the Armco iron cylinder.

The cylinders were stacked one on top of the other as shown in Figure 3-4

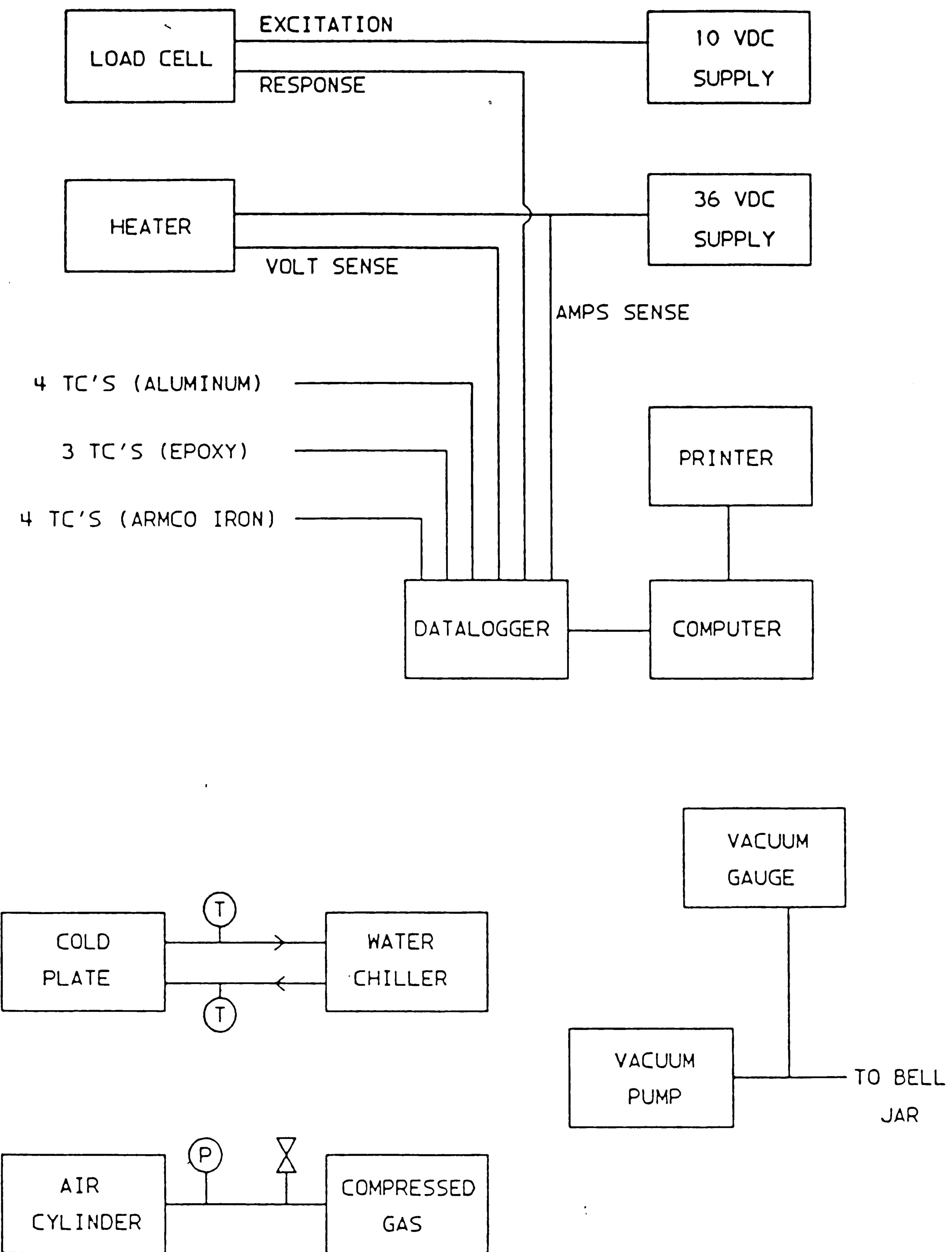

Figure 3-1: Schematic of thermal conductivity test apparatus

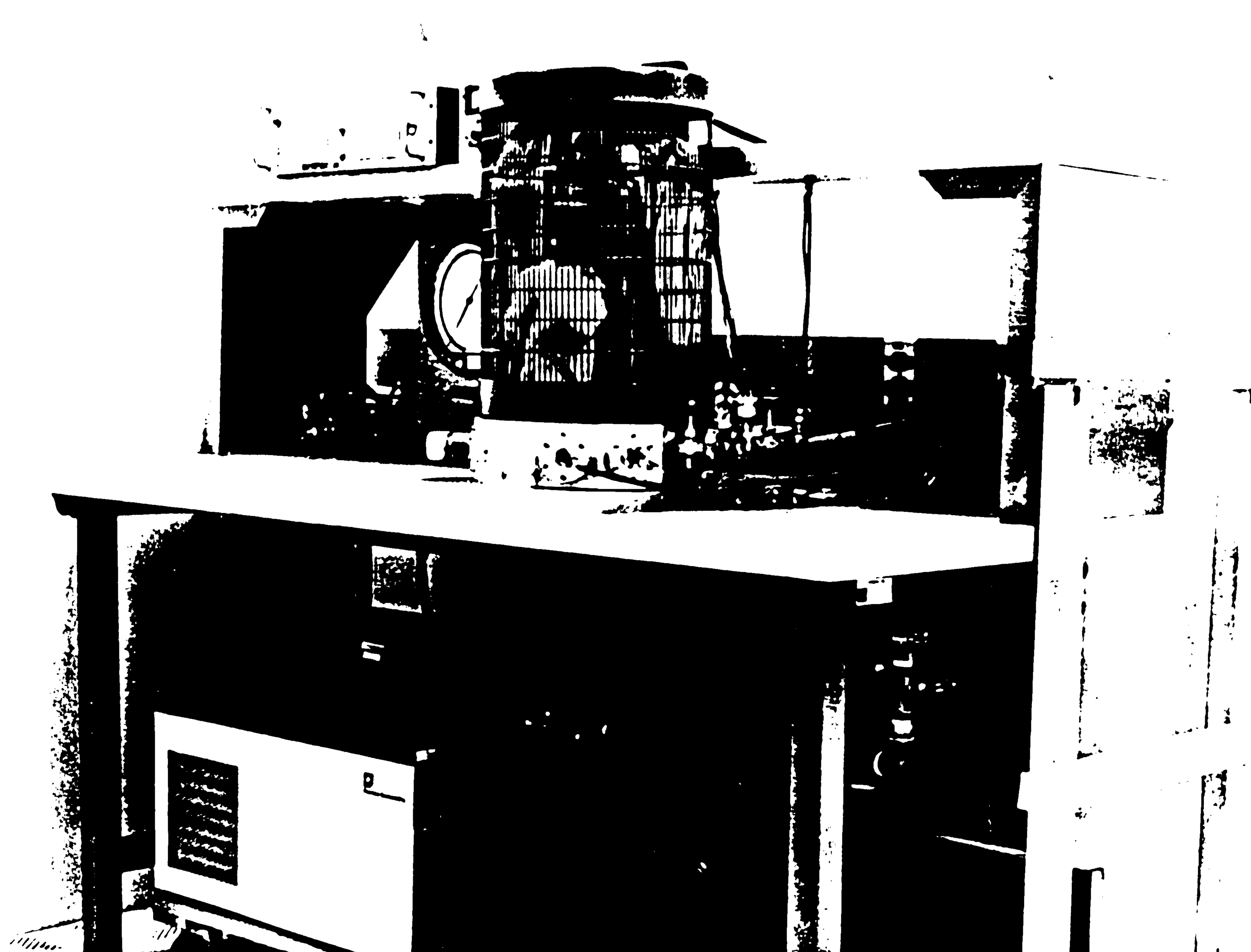

Figure 3-2: Photograph of thermal conductivity test area

and then adjusted to align them all on one axis. The heater and insulation disks were placed on top of the aluminum cylinder. A steel ball was placed between the air cylinder pressure plate and the insulation disks. After double checking the alignment of all of the components in the column, the regulator was opened slightly, thereby placing the column in compression. The pressure reduced the interfacial resistances and prevented the cylinders from shifting. The pressure was regulated to approximately 4000 kg/m^2 for all test runs.

A small amount of heat sink compound was applied to the tips of three copper-constantan thermocouples. The thermocouples were encased in a 0.51 mm diameter stainless steel sheath. The thermocouples were then inserted into the epoxy specimen holes which are numbered five through seven in Figure 3-3.

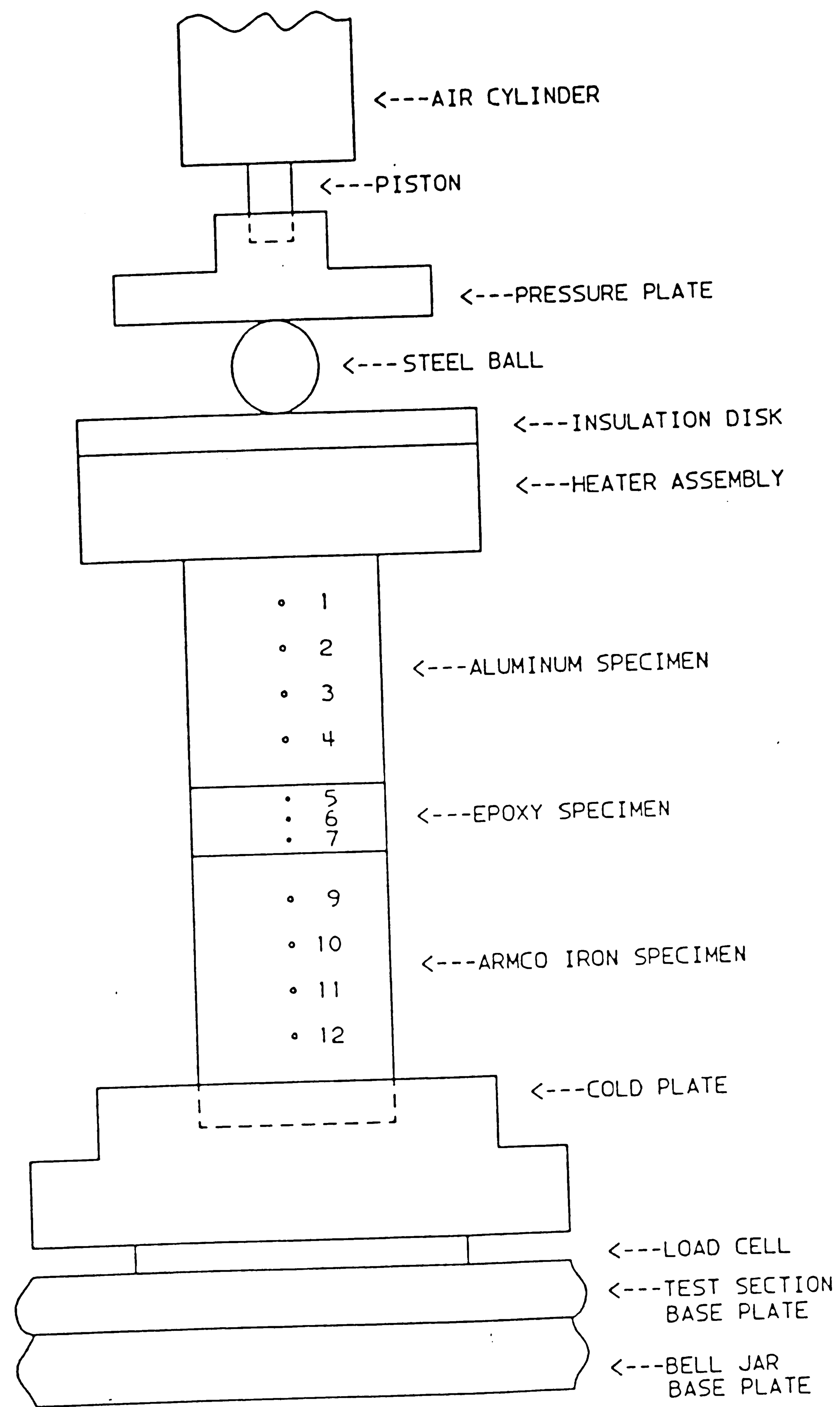

Figure 3-3: Schematic of test column

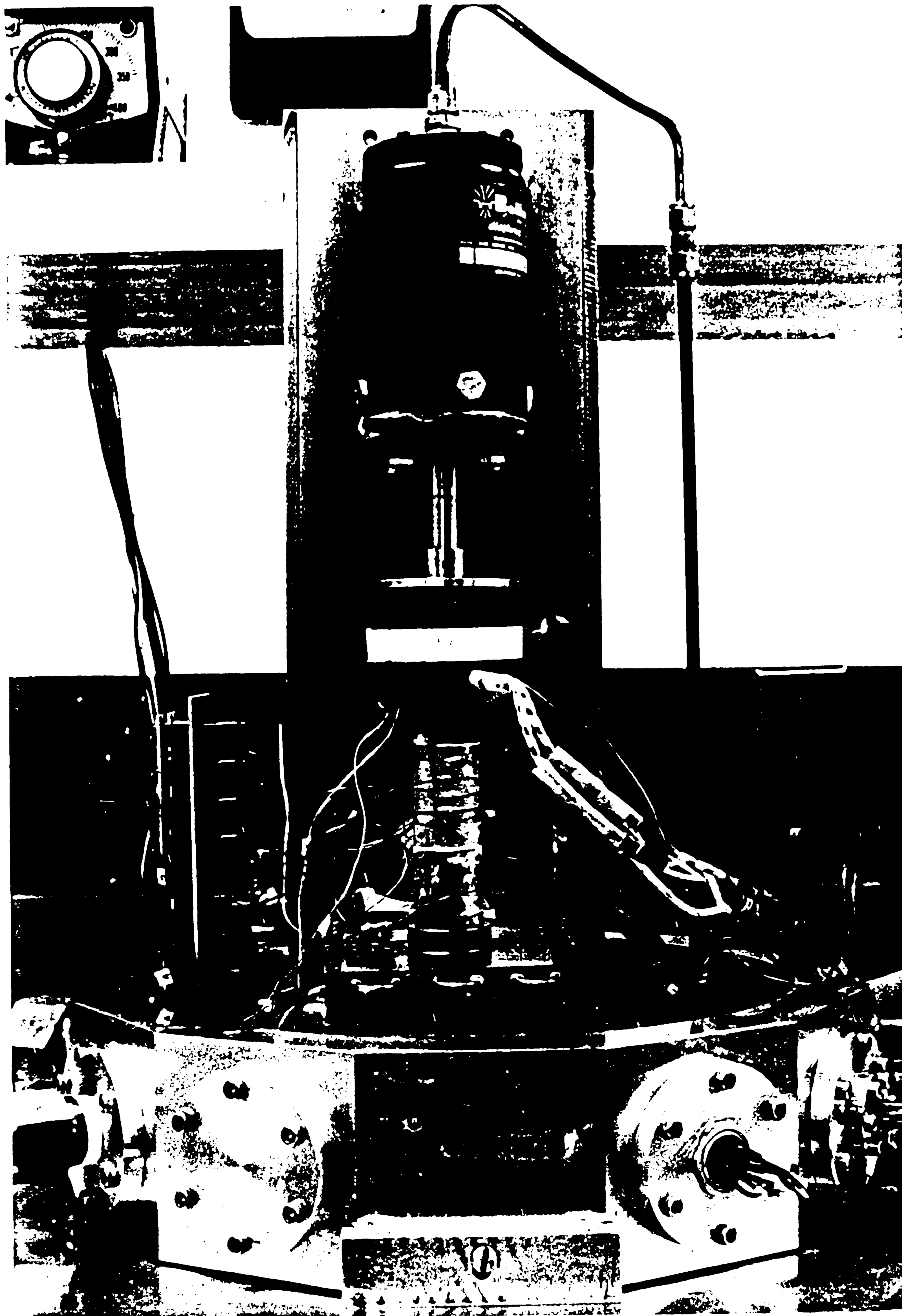

Figure 3-4: Photograph of test column
Note the relative position of the heater, aluminum cylinder, epoxy specimen, Armco iron cylinder and cold plate

It was not necessary to place thermocouples into the Armco iron specimen as these thermocouples and the Armco iron cylinder itself are considered to be permanent components of the test rig. These thermocouple holes are labelled nine through twelve in Figure 3-3. The number eight thermocouple was of the type used in the epoxy cylinder, but it was not inserted into the column. Instead, it measured the ambient temperature inside the test chamber.

A 13 mm thick glass-filled insulation, Cotronics 370-3, was wrapped around the test column and secured to itself with tape. This insulation reduced the heat lost from the column.

To reduce the possibility of a vacuum leak, a very thin layer of Dow Corning high vacuum grease was applied to the bell jar gasket. The bell jar was then lowered onto the base of the test rig. After aligning the bell jar properly, the vacuum pump was turned on.

3.2 Software preparation

The Fluke datalogger, the printer, the computer, and the expansion unit were powered up. The program "Contact" was loaded up at the pc and the test parameters were changed by typing the line number, followed by the new parameters. The specimen number and a very brief description of the run were entered as comments. After inputting the necessary data, the test parameters were printed.

3.3 Making a test run

The heater power supply was activated and water chiller temperature was set to 5.0°C. After checking to see that these systems were operating properly, the test was started from the pc. As the test ran, it was necessary to adjust the heater voltage so that the top of the epoxy cylinder did not exceed 70°C. The heater setting was different for each specimen. The program monitored the temperatures at each of the thermocouples and, once the steady state criteria had been met, displayed a statement indicating this condition. The steady state test results were then printed.

Chapter 4
RESULTS AND DISCUSSION

The specimens tested in the thermal conductivity rig are shown in Figure 4-1. The specimens varied in color as a function of the loading of boron nitride and the curing agent which was selected. Figure 4-2 is a close-up view of a typical specimen; #95.

Figure 4-1: Photograph of test specimens

4.1 Retention of dimensions

Table C-1 reports the thickness of each specimen prior to and after testing. The thickness of two of the specimens was reduced during testing. Specimen #52 was 0.10 mm thinner and specimen #70 was 0.01 mm thinner after test.

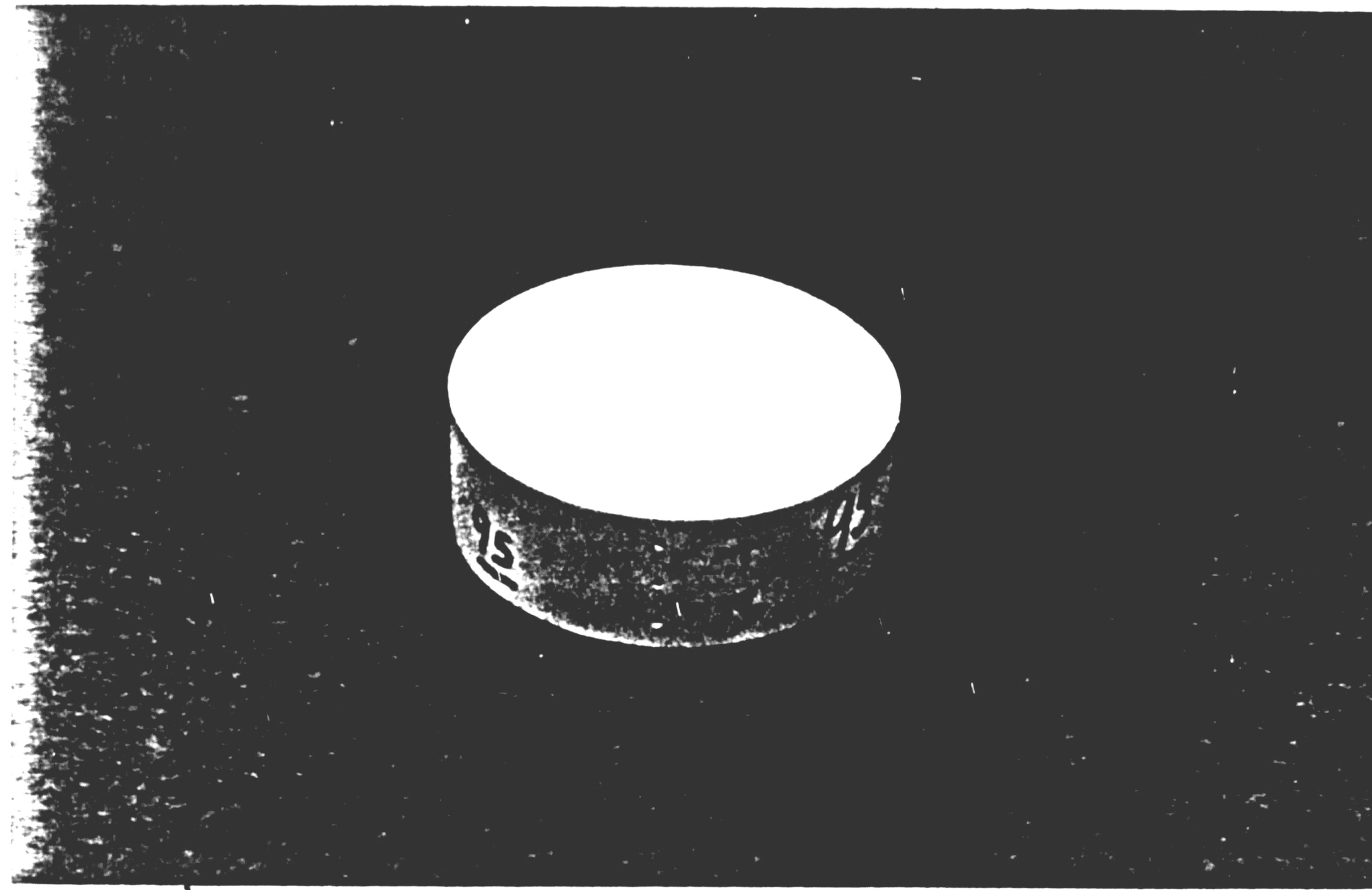

Figure 4-2: Photograph of specimen #95

It was obvious what happened to specimen #52, the first, or "trial run" specimen[2]. During the test the temperature of the aluminum cylinder reached 80°C. This temperature, coupled with the compressive stress placed on the specimen, was high enough to cause a reduction in the specimen thickness. A photograph of this specimen appears in Figure 4-3.

---

[2]Specimen #52 differed from the rest of the specimens as it was not postcured and was machined to a thickness of 10.80 mm.

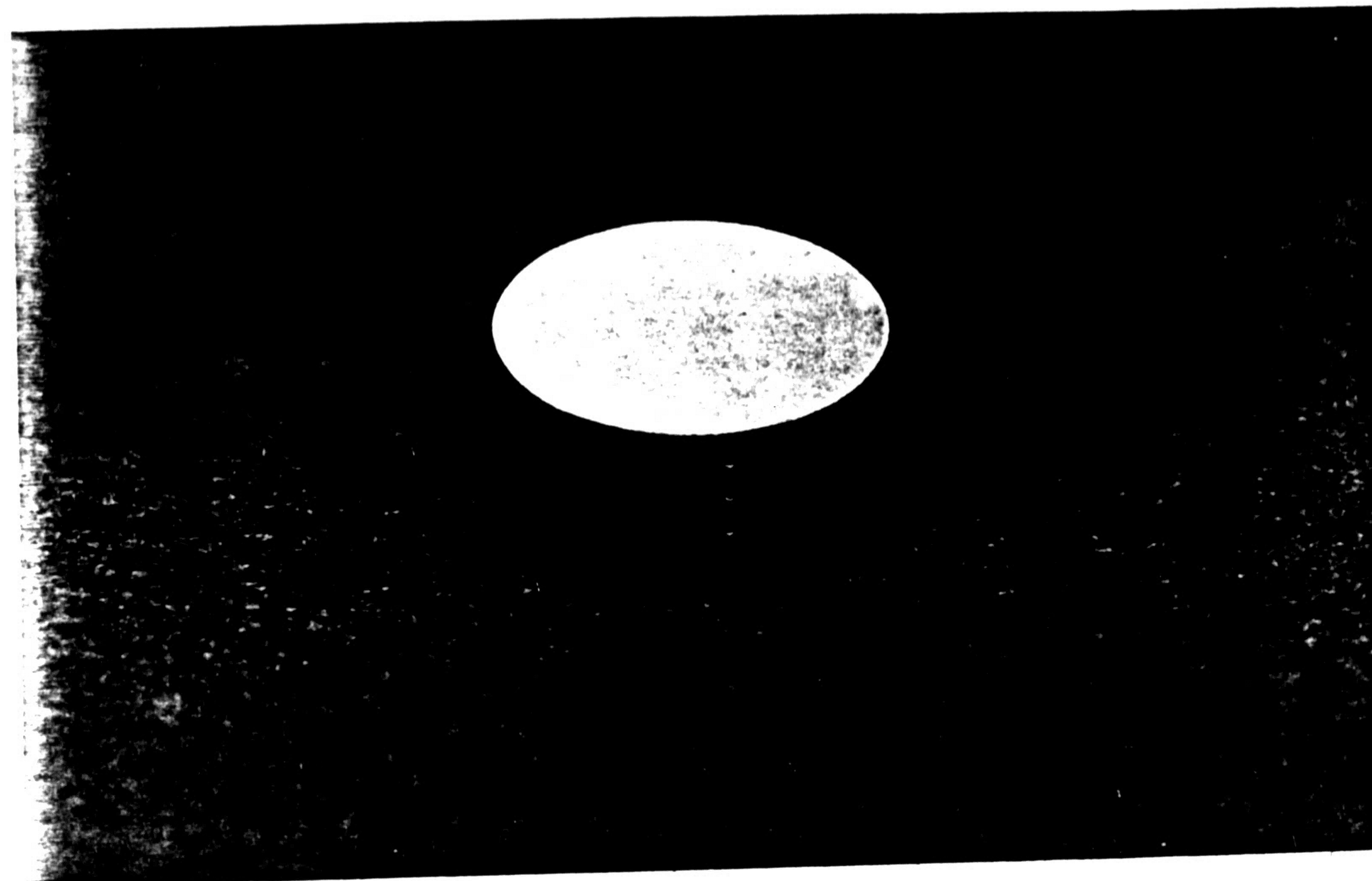

Figure 4-3: Photograph of specimen # 52

As a result of this experience, a 100°C postcure was implemented as it was expected that a high temperature postcure would increase the heat deflection temperature of the specimens. Additionally, the temperature of thermocouple number four was monitored and the heater voltage was adjusted to prevent the temperature from exceeding 70°C. While probably not as crucial, the pressure on the column was regulated to approximately 4000 kg/m^2 to reduce the chance of "squashing". No dramatic reductions in specimen thickness occurred after these additional test procedures were implemented.

Specimen #70 measured 0.01 mm thinner after testing. No explanation can be offered as to why the specimen might have become thinner as a result of the test. However, it is likely that the specimen thickness did not actually change and the apparent change was due to an error in measurement.

4.2 Thermal Conductivity Results

It was assumed that the heat which passed thru the epoxy cylinder was equal to the amount of heat passing thru the Armco iron cylinder. The thermal conductivity of the epoxy was calculated using this very conservative estimate of the heat flux thru the epoxy and using the temperatures indicated by the three thermocouples in the epoxy cylinder. These data, reported in Table C-2, have been rounded to the appropriate number of significant figures after performing the necessary calculations. This procedure was followed for the remainder of the data reported in the appendices.

Table C-3 reports the boron nitride loading and thermal conductivity of each specimen. Two values are listed for each specimen. The first was calculated using the mean of the four temperature gradients. The second, referred to in the table as the "vote" value, was calculated using the mean of the two least extreme temperature gradients. This is equivalent to ignoring the lowest and highest temperature gradients. This calculation was made to ensure that the results had not been influenced by an inaccurate thermocouple. As may be seen from Table C-3, the mean and vote values show good agreement, indicating that all four thermocouples performed about equally. Therefore, the discussions which follow are based on the mean thermal conductivity results.

Regression analysis produced the following equation to represent the thermal conductivity of the epoxy composite:

$$\lambda = 0.22 + 0.021\text{wt\%HCM} + 0.027\text{wt\%HCP} + 0.81\times10^{-6}(\text{wt\%HCP}+\text{wt\%HCM})^{3.6} + 0.013(\text{wt\%HCM}\times\text{wt\%HCP})^{0.6}$$

where:

λ = thermal conductivity of epoxy composite, $\frac{watts}{m\,^{o}K}$

wt% HC(M,P) = weight percent HC(M,P) boron nitride in the specimen.

This equation fits the data with a correlation coefficient of 0.98.

Table C-4 contains actual experimental and "predicted" thermal conductivity values. This equation was developed to fit the data taken here; it was not intended to (and probably would not) represent the system at loadings significantly above those tested here. For example, this equation "predicts" that a 70 wt% HCM boron nitride specimen would have a thermal conductivity of 5.2 watts/m °K. In reality, it is likely that the thermal conductivity would be greater due to the exponential increase in the number of conductive chains which form as the loading is increased.

Several observations may be made about this system. First, as expected, the thermal conductivity was strongly related to the loading; as the loading was increased, the thermal conductivity increased at a rate that exceeded linearity. The loading-thermal conductivity relationship is graphed in Figure 4-4. Second, the belief that the thermal conductivity would be maximized by a blend of the two powders was also substantiated by the results. While this work certainly does not offer proof, it does concur with the explanation that a blend has higher thermal conductivity because the smaller particles fill the interstices left by the larger particles, thereby increasing the particle to particle contact. Third, it was observed that the lowest thermal conductivity resulted when only boron nitride of the larger particle size was used. When one powder was used by itself, HCP resulted in greater values for thermal conductivity than HCM, but as mentioned previously, a blend was superior to either powder alone.

4.3 Evaluation of heat losses

Each run resulted in a "loss" of heat; that it, less heat flowed through the Armco iron specimen at the bottom of the column than had been generated by the heater at the top of the column. Several trial runs were performed to determine what testing procedures would minimize the heat losses. As may be seen from Table C-5, testing in a vacuum reduced heat losses. In addition, wrapping the test column with an insulating mat also reduced heat losses. As Table C-6 shows, the losses ranged from 15.7% to 50.7%, with a mean of 26.0%. Records were kept of the vacuum pressure during each run. Analysis of this data indicates that the heat loss is a function of both the vacuum pressure and the thermal conductivity of the specimen being tested. Losses were minimized when the vacuum pressure was low and the thermal conductivity of the specimen was high.

This relationship for the losses may be expressed as:

$$l = 32 + 0.071v - 4.9\lambda$$

where:

l = heat loss, %

v = vacuum pressure, μm Hg

λ = thermal conductivity of epoxy composite, $\frac{watts}{m\,^{o}K}$

Both of these results were expected. Testing in a vacuum reduces the heat lost to the environment surrounding the test column because the conductivity of air is negligible at pressures below 10^{-4} mm Hg[26]. Testing a specimen with high thermal conductivity reduces losses because less heat is conducted up the column, away from the epoxy cylinder.

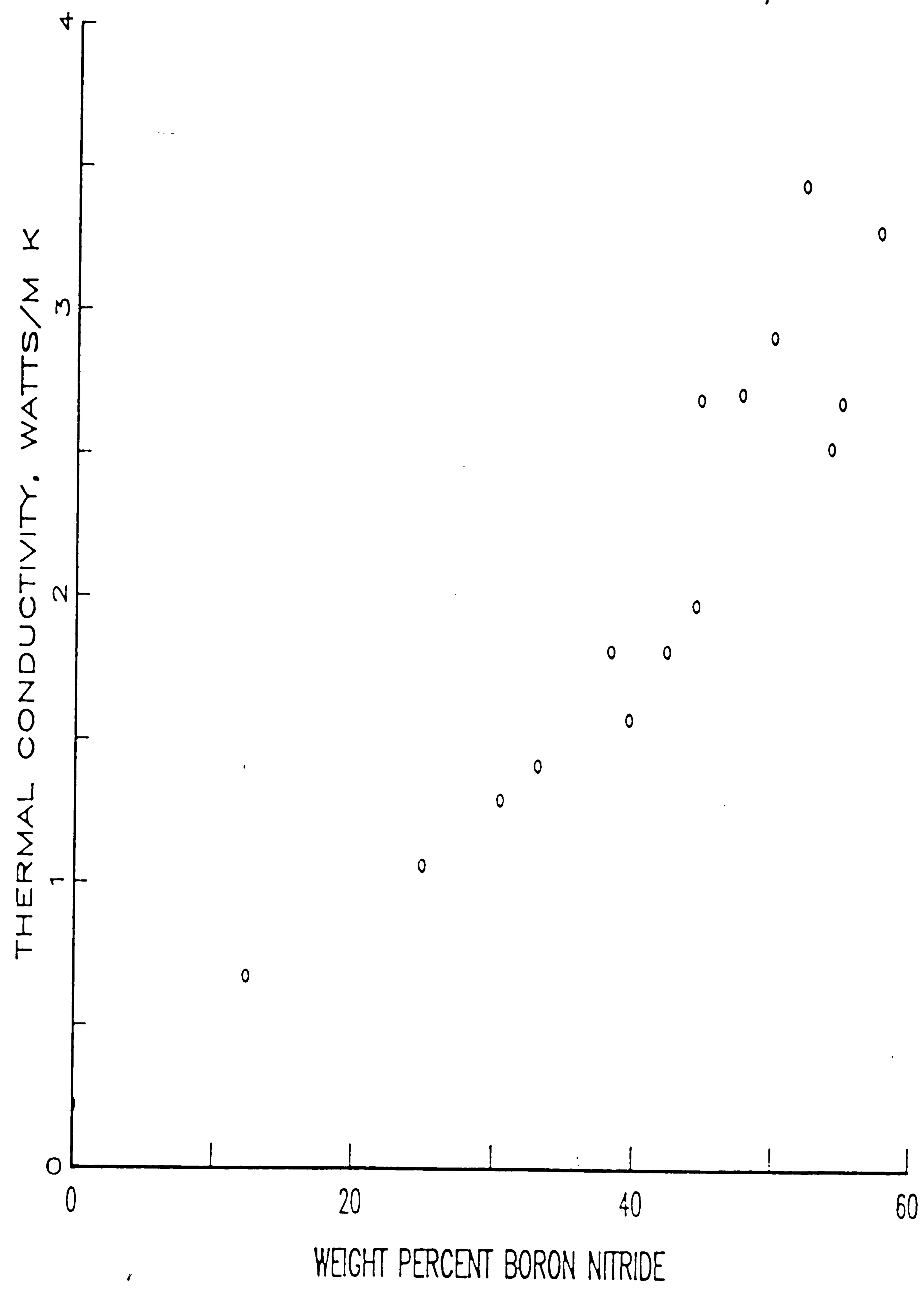

Figure 4-4: Thermal Conductivity vs. Loading of Boron Nitride

4.4 Specimen mass and density

Because boron nitride has a density of 2.26 g/cm^3, while the other components have densities in the range of 0.985 to 1.20 g/cm^3, the specimen density must increase as the loading is increased. The data in Table C-7 confirm that as the concentration of the boron nitride in the epoxy mixture was increased, the loading in the completed specimens also increased. This relationship is graphed in Figure 4-5. The specimen density increased linearly with the loading of boron nitride. This indicates that the test specimens were representative of the mixtures which were prepared, that is, what was measured into the beaker when the composite was being prepared actually ended up in the test specimen. The deviation from linearity is greatest at higher loadings, a result which probably occurred because mixing and casting the composite became more difficult as the loading was increased.

4.5 Comparison to Previous Work

Smith[27] has also examined the thermal conductivity of boron nitride filled epoxy composites. Appendix D reports the average thermal conductivity values which were obtained by analysis of his data. Smith used a thermal comparator to make the conductivity measurements. It is difficult to make direct comparisons between this work and Smith's work because each used different epoxy resins and different boron nitride powders. Smith's thermal conductivity values are slightly higher than those obtained in this work.

Besides the differences already mentioned, another possible reason for disagreement in the results is that the results reported here are based on a very conservative application of Fourier's equation by considering the heat flux to be that observed in the bottom (Armco iron) cylinder. This resulted in thermal

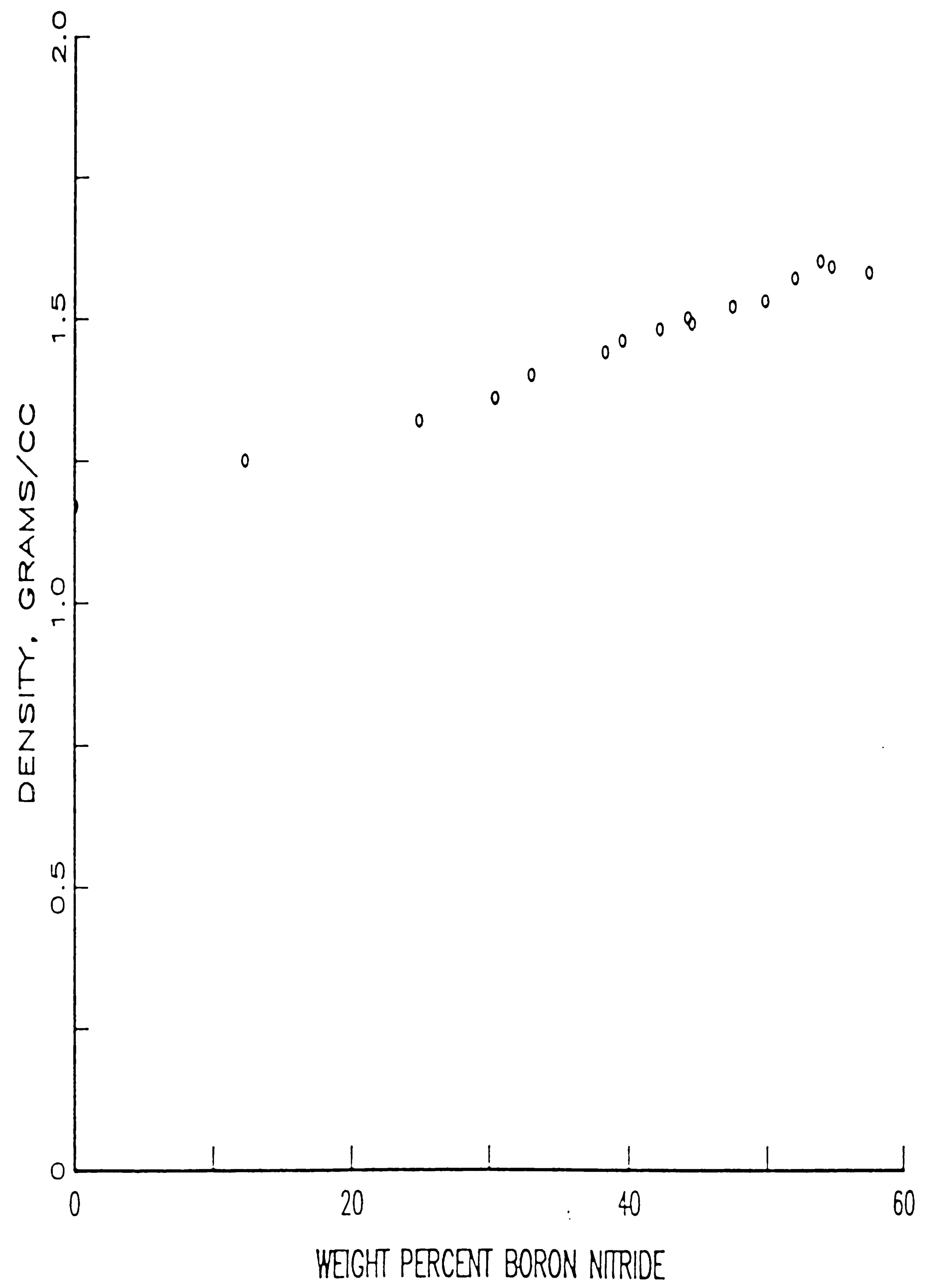

Figure 4-5: Specimen Density vs. Loading of Boron Nitride

conductivity values which are almost certainly on the low side. Higher thermal conductivity results would have been obtained if the calculations had instead been based either on the heat flux in the top (aluminum) cylinder, or on the average of the heat flux in the aluminum and Armco iron cylinders. Using specimen #73 as an example, the mean thermal conductivity calculated based on the heat flux in the Armco iron cylinder alone is 1.6 W/m °K. Calculations based on the average of the heat flux in the aluminum and Armco iron cylinders, and based on the heat flux in the aluminum cylinder alone, produce results of 1.8 and 2.0 W/m °K, respectively.

4.6 Suggestions for Future Work

Based upon experience gained by this work, the following suggestions for future work may be made:

1. Improve the heater design. The heater used in this work had a larger surface area than was actually needed, a factor which contributed to the heat losses. Since the completion of this project, tests performed using a redesigned heater have resulted in losses of 10% to 20%, well below the mean loss of 26% which was experienced in the work presented here.

2. Change the mold design. A number of specimens were cast that were never used, due to unacceptable porosity. Since these castings were made at atmospheric pressure, applying pressure to a vented mold should reduce porosity.

3. Grade the boron nitride powder more tightly. The typical screen analysis provided by the supplier does not give a very good idea of the particle size distribution. Reducing the variance of the particle size will increase repeatability and will also make the system a better candidate for modeling.

4. Modify the test procedure to permit measurement of the interfacial resistance between the epoxy and a second surface, for example, aluminum. The bulk thermal conductivity which was determined by this work is only one important thermal characteristic. As the joint thickness is decreased, the interfacial resistance becomes increasingly important. In fact, the interfacial resistance can become the dominant factor in the system. This work is in progress.

5. Determine the dielectric strength of the epoxy composites. A goal of this project was to develop a thermally conductive, electrically insulating epoxy composite. It is believed that the formulations tested do have sufficient dielectric strength as all of the components are electrically insulating, however, data must be gathered to support this conclusion.

6. Perform mechanical tests to determine if this system can be used in applications requiring zero fails per 100,000 hours of operation. Resistance to thermal cycling will be an important consideration.

Chapter 5
Models of Thermal Conductivity of Composite Systems

This chapter examines several models designed to predict the thermal conductivity of composite systems. Some models function independent of the filler geometry and are based only on the volume fraction of filler and the thermal conductivities of the two phases. Included in this group of models are the rule of mixtures, the inverse rule of mixtures, and the geometric mean model.

As Nielsen discusses,[28, 29] a model should not only consider the thermal conductivity of the two components and their concentrations, but also the size, shape and packing characteristics of the filler. As the concentration of the filler approaches the maximum packing fraction, the thermal conductivity should increase at an increasing rate because of the exponential growth in the number of particle to particle contacts which create paths for easy heat flow. Unfortunately, many models ignore this phenomenon and assume that the thermal conductivity will change linearly over the entire range of filler concentration.

Lewis and Nielsen have developed a semi-theoretical model which, as Nielsen demonstrates, can be used to characterize a number of systems. These systems include aluminum spheres in rubber, aluminum cylinders in rubber, graphite fibers in epoxy, magnesium oxide in polystyrene, magnesium oxide in polyethylene, glass spheres in polystyrene, and glass spheres in polyethylene. In each of the systems considered, the Lewis and Nielsen model correlates well with the experimental results.

Models which consider the filler geometry often assume that the variance about the mean particle size is negligible. Unfortunately, the boron nitride powders considered in this work were irregular in both size and shape. These characteristics of the powders made using the more sophisticated models virtually impossible.

This section discusses the application of a number of models to the boron nitride powder filled epoxy composite system. The models were used to predict the thermal conductivity of the system over a range of filler concentrations. The thermal conductivity of the continuous phase was taken to be 0.22 W/m °K as this is the thermal conductivity of the primary component, the resin. The thermal conductivity of the filler was taken to be 41.5 W/m °K as this is mean 38°C thermal conductivity of the boron nitride measured parallel and perpendicular to the pressing direction[5]. Each model's thermal conductivity predictions, expressed in units of W/m °K, will now be presented. The volume fraction boron nitride in each specimen is given in Table C-8.

5.1 Classical Models

All of the models make use of the following variables: the thermal conductivities of the continuous phase, the discrete phase or filler, and the composite, λ_1, λ_2, and λ, respectively. The volume fraction of the filler is V_f .

5.1.1 Rule of Mixtures

5.1.1.1 Equation used to model system

$$\lambda = (1-V_f)\cdot\lambda_c + (V_f\cdot\lambda_d)$$

5.1.1.2 Performance of the model

As is shown by Table E-1, this model consistently overestimated the thermal conductivity of the system. At loading of 55.0 wt% BN, the series model predicts a thermal conductivity of 16 as compared with the experimental result for specimen #70 of 2.7.

5.1.2 Inverse rule of mixtures

5.1.2.1 Equation used to model system

$$\frac{1}{\lambda} = \frac{(1-V_f)}{\lambda_c} + \frac{V_f}{\lambda_d}$$

5.1.2.2 Performance of the model

As is shown by Table E-1, this model consistently underestimated the thermal conductivity of the system. At 55.0 wt% boron nitride (specimen #70), the series model predicts a thermal conductivity of 0.36 while the experimental result was 2.7.

5.1.3 Geometric Mean Model

5.1.3.1 Equation used to model system

$$\lambda = (\lambda_d^{V_f})(\lambda_c^{[1-V_f]})$$

5.1.3.2 Performance of the model

As is shown by Table E-1, this model consistently underestimated the thermal conductivity of the system. The series model predicts a thermal conductivity of 1.7 for 55.0 wt% boron nitride, while the experimental result was 2.7. However, this model fit the experimental data better than did either the rule of mixtures model or the inverse rule of mixtures model.

5.2 Newer Models

A review article by Progelhof, Throne, and Ruetsch[30] provides an excellent overview of a number of these models.

5.2.1 Maxwell Theoretical Model

Source: reference 31.

5.2.1.1 Equation used to model system

$$\lambda = \frac{[2\lambda_1 + \lambda_2 + 2V_f(\lambda_2 - \lambda_1)]\lambda_1}{2\lambda_1 + \lambda_2 - V_f(\lambda_2 - \lambda_1)}$$

5.2.1.2 Performance of the model

As is shown by Table E-2, this model consistently underestimated the thermal conductivity of the system. Maxwell's model predicts a thermal conductivity of 0.63 for 55.0 wt% boron nitride, while the experimental result was 2.7.

5.2.2 Bruggeman Theoretical Model

Source: reference 32.

5.2.2.1 Equation used to model system

$$1 - V_f = \frac{\lambda_2 - \lambda}{\lambda_2 - \lambda_1} \cdot \left(\frac{\lambda_1}{\lambda}\right)^{[1/3]}$$

5.2.2.2 Performance of the model

As is shown by Table E-2, this model consistently underestimated the thermal conductivity of the system. Bruggeman's model predicts a thermal conductivity of 0.91 for 55.0 wt% boron nitride, while the experimental result was 2.7.

5.2.3 Lewis and Nielsen Semi-Theoretical Model

Source: references 28, 29, and 33.

5.2.3.1 Equation used to model system

$$\lambda = \lambda_1 \frac{1 + AV_f\left(\frac{\lambda_2/\lambda_1 - 1}{\lambda_2/\lambda_1 + A}\right)}{1 - \left[V_f\left(\frac{\lambda_2/\lambda_1 - 1}{\lambda_2/\lambda_1 + A}\right)\left(1 + \left(\frac{1 - S_m}{S_m^{\ 2}} V_f\right)\right)\right]}$$

A = shape factor

S_m = maximum packing fraction

5.2.3.2 Performance of the model

This model was not used because shape and packing factors were not available for the boron nitride powders.

5.2.4 Cheng and Vachon Theoretical Model

Source: references 34 and 35.

5.2.4.1 Equation used to model system

$$\frac{1}{\lambda} = \frac{1}{\{C(\lambda_2-\lambda_1)[\lambda_1+B(\lambda_2-\lambda_1)]\}^{1/2}} \cdot \ln \frac{[\lambda_1+B(\lambda_2-\lambda_1)]^{1/2}+B/2[C(\lambda_2-\lambda_1)]^{1/2}}{[\lambda_1+B(\lambda_2-\lambda_1)]^{1/2}-B/2[C(\lambda_2-\lambda_1)]^{1/2}} + \frac{1-B}{\lambda_1}$$

$$B = \left(\frac{3V_f}{2}\right)^{1/2}, \quad C = 4\left(\frac{2}{3V_f}\right)^{1/2}$$

5.2.4.2 Performance of the model

As is shown by Table E-2, this model consistently underestimated the thermal conductivity of the system. The Cheng and Vachon model predicts a thermal conductivity of 0.86 for 55.0 wt% boron nitride, while the experimental result was 2.7.

5.2.5 Agari and Uno Theoretical Model

Source: reference 36.

5.2.5.1 Equation used to model system

$$\lambda = \frac{[2\lambda_1 + \lambda_2 + 2V_{af}(\lambda_2 - \lambda_1)]\lambda_1}{2\lambda_1 + \lambda_2 - V_{af}(\lambda_2 - \lambda_1)} + V_f[V_f^{(V_f - 2/3)}]C^2\lambda_2$$

This model defines the following additional terms:

V_f = percentage of particles contributing to the formation of conductive chains.

V_{af} = percentage of particles not contributing to the formation of conductive chains.

C^2 = geometric factor which connects the observable conductivity with the random assembly of conductive chains.

5.2.5.2 Performance of the model

There exists a difficulty in using this model; while the volume fraction boron nitride in the specimen may be known, it is not known what fraction of the boron nitride particles forms conductive chains and what fraction does not. The authors suggest assuming values for V_f and V_{af}, however, to do so would eliminate the very purpose for which a model is sought - to predict the thermal conductivity of the system. As a consequence, this model was not used.

5.2.6 Hamilton and Crosser Semi-Theoretical Model

Source: reference 37.

5.2.6.1 Equation used to model system

$$\lambda = \lambda_1 \left[\frac{\lambda_2 + (n-1)\lambda_1 - (n-1) V_f (\lambda_1 - \lambda_2)}{\lambda_2 + (n-1)\lambda_1 + V_f (\lambda_1 - \lambda_2)} \right]$$

where n is a constant related to the shape of the filler. The definition of n is n = 3/Ψ, where Ψ is the sphericity. The sphericity is given by the ratio of two surface areas as: Ψ = surface area of sphere of volume equal to the filler particle/surface area of the particle.

5.2.6.2 Performance of the model

In order to apply this model to the boron nitride epoxy system, it was would be necessary to calculate the sphericity, a task which requires that the particles be of uniform shape and size. Unfortunately, the boron nitride particles are extremely irregular, eliminating any hope of calculating the sphericity. Therefore, this model could not be used.

5.3 Summary of Models

A number of models of thermal conductivity have been examined in this chapter. Of the classical models, the geometric mean model performed best; of the more complex models, Bruggeman's model demonstrated the best performance. None of the models performed well enough to be able to say that the model was a good representation of the system.

There are a number of possible explanations for why this system was such a poor candidate for modeling. As discussed earlier, the geometry of the boron nitride particles (irregular hexagonal plates) makes it difficult to develop values for shape and packing factors. The wide distribution in particle size within each powder type, and then the introduction of two different powders added greatly to the complexity of the system. Perhaps of greatest importance is a variable which was overlooked by the models considered here. This factor is the interfacial resistance which occurs between individual boron nitride particles and the epoxy resin. It seems reasonable to expect that the interfacial resistance will have a large influence on the thermal conductivity of the composite, especially when the loading is low enough that conduction via chains of particles only makes a small contribution to the overall thermal conductivity of the composite.

Chapter 6
CONCLUSIONS

1. The thermal conductivity was strongly related to the loading of boron nitride. The results are similar to those of Smith[27].
A number of models of thermal conductivity were considered, however, several could not be used because of the highly irregular shape and size of the boron nitride powders. Those models which could be applied to this system failed to represent it well. As a result, an empirical equation was developed to model the thermal conductivity of the system. This equation is:

$$\lambda = 0.22 + 0.021 \times \text{wt\%HCM} + 0.027 \times \text{wt\%HCP} +$$

$$0.81 \times 10^{-6}(\text{wt\%HCP} + \text{wt\%HCM})^{3.6} + 0.013(\text{wt\%HCM} \times \text{wt\% HCP})^{0.6}$$

where:

λ = thermal conductivity of epoxy composite, $\frac{watts}{m\,^{o}K}$

wt% HC(M,P) = weight percent HC(M,P) boron nitride in the specimen.

This equation fits the data with a correlation coefficient of 0.98.

2. The test apparatus and procedures used in this work offer an alternative to other techniques, such as the use of a thermal comparator, for determining the thermal conductivity of a composite material.

3. This test method may have some repeatability advantages over a thermal comparator.

4. This test method requires considerably more time and effort than does a thermal comparator.

Appendix A
Description of test apparatus

The test apparatus was built by Vince Antonetti as part of his PhD thesis on thermal contact conductance. The description of the test apparatus which follows is essentially unchanged from his thesis[38]. The apparatus is similar to that discussed by Mirkovich[39] and Tye[40].

The heart of the apparatus is the test column, which is supported by a stainless steel support structure and is housed in a bell jar. An air cylinder, a heater block, and a water-cooled cold plate also mount to the support structure. The air cylinder is used as the loading mechanism. Heat flows from the heater at the top of the column, through the aluminum cylinder, the epoxy cylinder, and the Armco iron cylinder and finally into the cold plate at the bottom of the column.

The air cylinder located within the vacuum chamber allowed an axial force to be applied by adjusting the pressure of an external compressed gas source. The combination of the nearly frictionless diaphragm-type air cylinder and the large reservoir between the air cylinder and the pressure regulating valve allowed thermal expansion of the test column to occur without large changes in the load. To assure that the loading was uniform, the force was applied to the test column through a 13 mm steel ball. The stress was measured by a gauge located at the pressure regulating valve.

Heat was provided by a 200 watt, cartridge-type heater which was silver epoxied into a cylindrical copper block. The heater was powered by a 36 volt dc power supply. To prevent the heater block from tarnishing, a thin layer of gold was vapor-deposited on the block where the copper contacted the upper

cylinder in the test column. At the other end of the column was a copper cold plate cooled by a closed-loop water chiller system. The heat load was measured at two locations: First, the input electrical power was calculated by monitoring the voltage drop across a precision resistor in series with the heater. Second, the heat flux through the Armco iron specimen was calculated by substituting the temperature gradient into Fourier's equation.

A two-stage mechanical pump was used to evacuate the bell jar. Because the conductivity of air decreases with decreasing pressure, heat losses were minimized by testing in a vacuum.

A Fluke datalogger, under the control of an IBM XT personal computer, scanned and read the thermocouple voltages, the load cell output voltage, and the heater voltage.

Appendix B
Equipment used in this project

B.1 Specimen preparation and inspection

1. Scales for weighing components and specimens: Mettler H20T and Mettler PC400

2. Micrometer for measuring specimen thickness: 25.4 mm capacity, Model M865-1, Mitutoyo Co., Japan

3. Atmospheric oven: Isotemp atmospheric oven, Junior Model, Fisher Scientific, Springfield, New Jersey

4. Mechanical blending apparatus: Dispersator Model, Premier Mill Corp., Temple, Pennsylvania

5. Vacuum oven: Model 5851-4, National Appliance Co., Portland, Oregon

6. Vacuum pump: Duo-Seal Model 1400, Sargent-Welch Scientific Co., Skokie, Illinois

7. Diamond saw for cutting castings to 10.0 mm thickness: Isomet Model, Buehler Inc., Lake Bluff, Illinois

B.2 Test Apparatus

1. Chiller: bath and circulator, Model 2067, Forma Scientific, Marietta, Ohio

2. Vacuum pump: two-stage, mechanical pump, 1 HP motor, Model 1397B, Sargent-Welch Scientific Co., Skokie, Illinois

3. Vacuum gauge: Thermopile type, Model DV-6, Teledyne Hastings, Hampton, Virginia

4. Power supply for heater: 0 to 36 DC volts, +/- 0.02% regulation, 0 to 10 amps, Model 809A, Harrison Labs, Berkeley Heights, New Jersey

5. Multimeter for heater current and voltage: Accuracy +/- 0.04% of reading, digital output, Model 8010A, John Fluke Manufacturing Co., Seattle, Washington

6. Precision resistor for heater current: 1.0 Ω +/- 1.0%, 100 watts, Dale RH-100

7. Cartridge heater: 1.3 cm diameter, 5 cm long, 24 volts DC, 200 watts, Watlow Manufacturing Corp., St. Louis, Missouri

8. Pressure gauge: 0 to 100 psi +/- 0.1%, Heise Co., Newton,

Connecticut

9. Air cylinder: Diaphragm type, no return spring, Model S4FBPFM modified, Bellofram Corp., Burlington, Massachusetts

10. Load cell: 0 to 500 lbs., bonded foil strain gage type, 10 volt excitation, 2 mv/volt output, temperature compensated, Sensotec Corp., Columbus, Ohio

11. Power supply for load cell: 0 to 20 volts, +/- 0.01% regulation, 0 to 1 amp, Model 611A, Harrison Labs, Berkeley Heights, New Jersey

12. Multimeter for load cell output voltage: accuracy +/- 0.02% of reading, Model HP 3465A, Hewlett Packard Co., Palo Alto, California

13. On/Off limit controller: Model 50, Omega Engineering, Inc., Stamford, Connecticut

14. Vacuum gauge: Hastings DV-6 gauge tube

15. Thermocouple for epoxy specimen: copper-constantan, 0.51 mm diameter 304 stainless steel sheath, Catalog Number SCPSS-020G-6, Omega Engineering, Inc., Stamford, Connecticut

16. Thermocouple for aluminum and Armco iron cylinders: copper-constantan, 0.13 mm diameter, bare wire type, Catalog Number COCO-005, Omega Engineering, Inc., Stamford, Connecticut

17. Datalogger: Model 2280B, John Fluke Manufacturing Co., Seattle, Washington

18. Apparatus control units: IBM Personal Computer XT and IBM Expansion Unit

Appendix C
Data

Specimen number	Thickness (mm) before testing	after testing	Δ
52	10.80	10.70	-0.10
57	9.53	9.53	0.00
61	9.53	9.53	0.00
62	9.53	9.53	0.00
63	9.53	9.53	0.00
64	9.53	9.53	0.00
65	9.53	9.53	0.00
68	9.53	9.53	0.00
70	9.53	9.52	-0.01
73	9.53	9.53	0.00
74	9.53	9.53	0.00
75	9.53	9.53	0.00
94	9.53	9.53	0.00
95	9.53	9.53	0.00
102	9.53	9.53	0.00

Table C-1: Specimen Thickness

Specimen number[3]	Q (W/m^2)	ΔT_1 (°K)	ΔT_2	λ_1 (W/m °K)	λ_2
52t	2,600	11.6	11.6	0.65	0.65
52b	2,800	11.8	11.3	0.68	0.71
57t	5,900	15.5	15.7	1.1	1.1
57b	5,900	16.5	15.6	1.0	1.1
61t	8,100	16.5	16.6	1.4	1.4
61b	8,100	16.6	15.5	1.4	1.5
62t	9,600	15.1	15.5	1.8	1.8
62b	9,300	15.2	13.9	1.7	1.9
63t	9,800	10.0	10.4	2.8	2.7
63b	9,100	9.9	9.9	2.6	2.6
64t	9,100	9.6	11.0	2.7	2.4
64b	10,000	10.0	10.7	3.0	2.8
65t	11,000	8.1	10.6	3.9	3.0
65b	12,000	10.6	10.2	3.3	3.5
68t	11,000	12.9	11.8	2.4	2.7
68b	11,000	11.9	14.2	2.7	2.3
70t	11,000	12.7	11.6	2.5	2.8
70b	11,000	11.9	12.2	2.7	2.7
73t	8,500	15.1	15.4	1.6	1.6
73b	8,500	16.1	15.4	1.5	1.6
74t	9,600	15.4	14.0	1.8	2.0
74b	9,100	15.7	14.3	1.7	1.8
75t	9,300	13.2	13.6	2.0	2.0
75b	9,900	14.5	14.6	2.0	1.9
94t	15,000	12.3	12.7	3.4	3.3
94b	14,000	13.5	11.6	3.0	3.4
95t	6,700	14.5	15.5	1.3	1.2
95b	7,300	15.6	16.1	1.3	1.3
102t	13,000	13.1	12.8	2.9	2.9
102b	13,000	12.9	12.0	2.8	3.0

Table C-2: Calculations of Thermal Conductivity

[3]Notation: t = specimen oriented same as when casting was made, b = specimen oriented opposite to when casting was made

Specimen Number	Loading (wt% boron nitride)			Thermal Conductivity (W/m °K)	
	HCM	HCP	total	mean	vote
0	0.0	0.0	0.0	0.22[4]	0.22
52	0.0	12.3	12.3	0.67	0.66
57	12.4	12.6	25.0	1.1	1.1
61	16.6	16.6	33.1	1.4	1.4
62	23.0	15.4	38.4	1.8	1.8
63	27.8	16.9	44.8	2.7	2.7
64	28.6	19.2	47.7	2.7	2.7
65	40.7	11.6	52.3	3.4	3.4
68	54.2	0.0	54.2	2.5	2.6
70	55.0	0.0	55.0	2.7	2.7
73	39.7	0.0	39.7	1.6	1.6
74	42.4	0.0	42.4	1.8	1.8
75	44.5	0.0	44.5	2.0	2.0
94	57.8	0.0	57.8	3.3	3.4
95	0.0	30.5	30.5	1.3	1.3
102	40.0	10.0	50.1	2.9	2.9

Table C-3: Thermal Conductivity versus Boron Nitride Loading

[4]Value supplied by resin manufacturer

Specimen Number	Thermal Conductivity (W/m °K) mean		vote	
	experimental	predicted[5]	experimental	predicted[6]
0	0.22	0.22	0.22	0.23
52	0.67	0.56	0.66	0.57
57	1.1	1.2	1.1	1.2
61	1.4	1.6	1.4	1.6
62	1.8	2.0	1.8	2.0
63	2.7	2.5	2.7	2.5
64	2.7	2.8	2.7	2.8
65	3.4	3.2	3.4	3.2
68	2.5	2.8	2.6	2.8
70	2.7	2.9	2.7	2.9
73	1.6	1.5	1.6	1.5
74	1.8	1.7	1.8	1.7
75	2.0	1.8	2.0	1.8
94	3.3	3.2	3.4	3.3
95	1.3	1.2	1.3	1.2
102	2.9	2.9	2.9	2.9

Table C-4: Experimental vs. Predicted Thermal Conductivity

[5] Values based on BMDP analysis of mean thermal conductivity data

[6] Values based on BMDP analysis of "vote" thermal conductivity data

Test Conditions	Heat Loss (%)
In air, no insulation	78.5
In vacuum, no insulation	62.8
In air, with insulation	57.6
In vacuum, with insulation	48.2

Table C-5: Heat Losses in Trial Runs of Specimen #52

Specimen number	Vacuum Pressure (μm Hg)	Heat Loss (%)
52t	80	50.7
52b	76	30.1
57t	27	27.7
57b	30	31.5
61t	30	20.5
61b	41	24.0
62t	30	29.1
62b	20	30.2
63t	55	24.1
63b	59	28.3
64t	80	22.9
64b	120	25.9
65t	72	21.4
65b	53	18.1
68t	66	23.1
68b	60	26.7
70t	34	25.4
70b	31	18.4
73t	50	25.7
73b	45	32.4
74t	34	25.2
74b	59	34.2
75t	48	24.5
75b	52	26.2
94t	45	17.2
94b	80	21.7
95t	56	34.4
95b	75	15.7
102t	66	22.6
102b	75	21.8

Table C-6: Heat Losses and Vacuum Pressure

Specimen number	Mass (grams)	Density ($\frac{g}{cm^3}$)
52	7.64[7]	1.25
57	8.06	1.32
61	8.53	1.40
62	8.78	1.44
63	9.12	1.49
64	9.31	1.52
65	9.56	1.57
68	9.80	1.60
70	9.74	1.59
73	8.92	1.46
74	9.03	1.48
75	9.16	1.50
94	9.67	1.58
95	8.28	1.36
102	9.36	1.53

Table C-7: Specimen Mass and Density

[7] normalized to 9.53 mm thickness

Specimen Number	Weight Percent Boron Nitride	Volume Percent Boron Nitride
0	0.00	0.00
52	12.3	6.81
57	25.0	14.6
61	33.1	20.5
62	39.4	24.5
63	44.8	29.5
64	47.7	32.1
65	52.3	36.3
68	54.2	38.4
70	55.0	38.7
73	39.7	25.6
74	42.4	27.8
75	44.5	29.5
94	57.8	40.4
95	30.5	18.4
102	50.1	33.9

Table C-8: Boron Nitride Volume and Weight Percent

Appendix D
Data from Previous Work

Loading (wt% boron nitride)	Thermocouple Output (μV)	Thermal Conductivity (W/m ^{o}K)
10	116	0.27
15	155	0.50
20	190	0.90
25	223	1.50
30	216	1.40
40	280	3.90

Table D-1: Thermal Conductivity Data of R. M. Smith

Appendix E
Results of Other Models

Specimen Number	Thermal Conductivity (W/m °K) Experimental	Series	Parallel	Geometric Mean
0	0.22	0.22	0.22	0.22
52	0.67	3.0	0.24	0.31
57	1.1	6.3	0.26	0.47
61	1.4	8.7	0.28	0.65
62	1.8	10.	0.29	0.79
63	2.7	12.	0.31	1.0
64	2.7	14.	0.32	1.2
65	3.4	15.	0.34	1.5
68	2.5	16.	0.36	1.6
70	2.7	16.	0.36	1.7
73	1.6	11.	0.30	0.84
74	1.8	12.	0.30	0.94
75	2.0	12.	0.31	1.0
94	3.3	17.	0.37	1.8
95	1.3	7.8	0.27	0.58
102	2.9	14.	0.33	1.3

Table E-1: Experimental Thermal Conductivity Compared to Series, Parallel, and Geometric Mean Models

Specimen Number	Thermal Conductivity (W/m °K) Experimental	Maxwell	Bruggeman	Cheng-Vachon
0	0.22	0.22	0.22	0.22
52	0.67	0.27	0.27	0.32
57	1.1	0.33	0.35	0.40
61	1.4	0.39	0.43	0.48
62	1.8	0.43	0.50	0.54
63	2.7	0.49	0.61	0.63
64	2.7	0.53	0.68	0.68
65	3.4	0.59	0.82	0.79
68	2.5	0.62	0.89	0.85
70	2.7	0.63	0.91	0.86
73	1.6	0.44	0.52	0.55
74	1.8	0.47	0.57	0.59
75	2.0	0.49	0.61	0.63
94	3.3	0.66	0.98	0.92
95	1.3	0.37	0.40	0.45
102	2.9	0.55	0.73	0.72

Table E-2: Experimental Thermal Conductivity Compared to Models by Maxwell, Bruggeman, and Cheng and Vachon

Appendix F
Description of Thermal Comparator

This section, based on the operations and maintenance manual for a thermal comparator[41], describes the theory behind the operation of a thermal comparator.

The thermal comparator registers the rate of cooling experienced by the tip of a heated probe upon contact with the surface of a material. The probe assembly consists of a sensing tip, heater and thermal reservoir. These components are held at an elevated temperature, T_1. The test specimen is at room temperature, T_2. The probe tip has thermal conductivity λ_1, while the test specimen has thermal conductivity λ_2. When the tip of the probe contacts the test specimen, its temperature drops to an intermediate temperature given by:

$$T_c = \frac{(T_1 \cdot \lambda_1) + (T_2 \cdot \lambda_2)}{\lambda_1 + \lambda_2}$$

The thermal comparator employs a thermocouple whose thermoelectric junction is near to the end of the sensing tip and is differentially connected with another junction located within the thermal reservoir. This differential reading is given by:

$$T_1 - T_c = \frac{\lambda_2 (T_1 - T_2)}{\lambda_1 + \lambda_2}$$

Maximum sensitivity and freedom from influence of pressure is obtained

when the thermocouple junction is at the contact interface, a condition that would require that the thermocouple be composed of the probe and the test specimen. Instead, the thermocouple is located as close to the tip as possible.

The user tests a number of samples whose thermal conductivity is known and plots the results on log-linear graph paper. Thermal conductivity is plotted on the linear scale, while emf is plotted on the log scale. A best-fit curve is drawn on the graph. This serves as the calibration curve. The emf of the unknown specimen is transferred to the calibration curve and the corresponding thermal conductivity located. It is important that the thermal conductivities of the calibration samples bracket the thermal conductivity of the unknown specimen.

REFERENCES

1. Specification Sheet for Epo-Tek H35-175M Electrically Conductive, Silver Epoxy. Epoxy Technology Inc., Billerica, Massachusetts

2. *Tabular Alumina Filled Casting Resin,* Cast-Coat Inc., Bridgewater, Massachusetts, 1986, Technical Data Sheet CC3-300

3. "Fisher Scientific 1986 Catalog". Fisher International, Springfield, New Jersey

4. *Boron Nitride Price Sheet,* Union Carbide Corp., Electronics, Specialty Products Group, 1986.

5. Koenig, J. R., "Evaluation of the Thermal Conductivity of Union Carbide Hot Pressed HBR Grade Boron Nitride", Tech. report, Southern Research Institute, Birmingham, Alabama, April 1981.

6. Kingery, W. D.; Bowen, H. K.; Uhlmann, D. R., *Introduction to Ceramics,* John Wiley and Sons, 1976.

7. Yao, Chingchi; Tzou, Joseph; Cheung, Robin; and Chan, Hugo, "Temperature Dependence of CMOS Device Reliability", *IEEE 1986 International Reliability Physics*, Electron Devices and Reliability Societies of the Institue of Electrical and Electronics Engineers, Institute of Electrical and Electronics Engineers, April 1986, pp. 175-182.

8. *UCAR Boron Nitride...For the performance you demand,* Union Carbide Corp., Electronics, Specialty Products Group, 1985, Brochure SP1001 2.5M1185

9. *Technical Information Bulletin - Typical Particle Size Distribution of HCM Grade Boron Nitride Powder,* Union Carbide Corp., Specialties and Services, Cleveland, Ohio, 1986.

10. *Technical Information Bulletin - Typical Particle Size Distribution of HCP Grade Boron Nitride Powder,* Union Carbide Corp., Specialties and Services, Cleveland, Ohio, 1986.

11. *Epon Resin Structural Reference Manual,* Shell Chemical Co., Houston, Texas, 1981, number SC:67-81

12. *Epon Resin 828 Technical Bulletin,* July ed., Shell Chemical Co., Houston, Texas, 1984, number SC:235-81.828

13. *Epon Resin 828 Technical Bulletin,* October ed., Shell Chemical Co., Houston, Texas, 1985, number SC:235-85.828

14. *General Guide: Formulating with DOW Epoxy Resins,* Dow Chemical Co., Midland, Michigan, 1986, Form Number 296-346-186

15. *Dow Liquid Epoxy Resins,* Dow Chemical Co., Midland, Michigan, 1983, Form Number 296-224-783R

16. *Formulating with DOW Epoxy Resins, Casting, Potting and Encapsulation,* Dow Chemical Co., Midland, Michigan, 1986, Form Number 296-363-1286

17. *A Guide to Dow Corning Silane Coupling Agents,* Dow Corning Corp., Midland, Michigan, 1985, Form Number 23-012B-85

18. *Information about Organofunctional Silanes,* Dow Corning Corp., Midland, Michigan, 1986, Form Number 23-184C-86

19. *Epon Curing Agent Z Technical Bulletin,* September ed., Shell Chemical Co., Houston, Texas, 1982, number SC:235-82.457

20. *IMICURE EMI-24 Curing Agent Technical Bulletin,* Air Products and Chemicals, Inc., Allentown, Pennsylvania, 1986, Form Number 120-603

21. *Technical Bulletin: Heloxy WC-68,* Wilmington Chemical Corp., Wilmington, Delaware, 1986, Form Number 12112

22. *Epon Resin 828 Technical Bulletin,* October ed., Shell Chemical Co., Houston, Texas, 1985, number SC:235-85.828

23. *Information about Antifoam Materials,* Dow Corning Corp., Midland, Michigan, 1984, Form Number 22-033A-84

24. *Miller-Stephenson Product Information for MS-115 Epoxy Stripper,* Miller-Stephenson Chemical Co., Inc., Danbury, Connecticut, 1986, Form Number 1043-12D/20

25. "Caplugs Product Protectors". Protective Closures Co., Inc., Caplugs Division, Buffalo, NY

26. Antonetti, Vincent W., *On The Use of Metallic Coatings to Enhance Thermal Contact Conductance,* PhD dissertation, University of Waterloo, 1983.

27. Smith, R. M., "Adhesion Enhanced Thermally Conductive Backseal Material", International Business Machines Corp., Burlington, Vermont

28. Nielsen, Lawrence E., "Thermal Conductivity of Particulate-Filled Polymers", *J. Appl. Polym. Sci.*, Vol. 17, 1973, pp. 3819-3820.

29. Nielsen, Lawrence E., "The Thermal and Electrical Conductivity of Two-Phase Systems", *Ind. Eng. Chem. Fundam.*, Vol. 13, No. 1, 1974, pp. 17-20.

30. Progelhof, R. C., Throne, J. L., and Ruetsch, R. R., "Methods for Predicting the Thermal Conductivity of Composite Systems: A Review", *Polym. Eng. Sci.*, Vol. 16, No. 9, 1976, pp. 615-624.

31. Maxwell, James Clerk, *A Treatise on Electricity and Magnetism,* Dover Publications, Inc., New York, New York, Vol. One, 1954, Ch. 9

32. Bruggeman, D., "Dielectric Constant and Conductivity of Mixtures of Isotope Materials", *Ann. Phys.*, Vol. 24, 1935, pp. 636.

33. Lewis, T. B. and Nielsen, L. E., "Dynamic Mechanical Properties of Particulate-Filled Polymers", *J. Appl. Polym. Sci.*, Vol. 14, 1970, pp. 1449-1471.

34. Cheng, S. C., and Vachon, R. I., "A Technique for Predicting the Thermal Conductivity of Suspensions, Emulsions, and Porous Materials", *Int. J. Heat Mass Transfer*, Vol. 13, 1970, pp. 537-546.

35. Cheng, S. C., and Vachon, R. I., "The Prediction of the Thermal Conductivity of Two and Three Phase Solid Heterogeneous Mixtures", *Int. J. Heat Mass Transfer*, Vol. 12, 1969, pp. 249-264.

36. Agari, Y., and Uno, T., "Thermal Conductivity of Polymer Filled with Carbon Materials: Effect of Conductive Particle Chains on Thermal Conductivity", *J. Appl. Polym. Sci.*, Vol. 30, 1985, pp. 2225-2235.

37. Hamilton, R. L., and Crosser, O. K., "Thermal Conductivity of Heterogeneous Two-Component Systems", *Ind. Eng. Chem. Fundam.*, Vol. 1, No. 3, 1962, pp. 187-191.

38. Antonetti, Vincent W., *On The Use of Metallic Coatings to Enhance Thermal Contact Conductance,* PhD dissertation, University of Waterloo, 1983.

39. Mirkovich, V. V., "Comparative Method and Choice of Standards for Thermal Conductivity Determinations", *J. Am. Ceram. Soc.*, Vol. 48, 1965, pp. 387-391.

40. Tye, Ronald P., "Factors Influencing Thermal Conductivity Measurements on Composites", *High Temp.-High Pressures*, Vol. 17, 1985, pp. 311-316.

41. *Operation and Maintenance Manual for TC-1000 Thermal Comparator,* Lafayette Instrument Co., Lafayette, Indiana, date of publication unknown.

42. The Regents of the University of California, *BMDP Statistical Software Manual,* University of California Press, Berkeley, California, 1983, W. J. Dixon, Chief Editor

43. Weast, Robert C., Editor-in-Chief, *Handbook of Chemistry and Physics,* CRC Press, Inc., Boca Raton, Florida, 1984.

44. Potter, W.G., *Uses of Epoxy Resins,* Chemical Publishing Co., New York, 1975.

45. Lee, Henry and Neville, Kris, *Epoxy Resins - Their Applications and*

Technology, McGraw-Hill Book Co., Inc., 1957.

46. Lee, Henry and Neville, Kris, *Handbook of Epoxy Resins,* McGraw-Hill Book Co., Inc., 1967.

47. Geiger, G.H and Poirier, D.R., *Transport Phenomena in Metallurgy,* Addison-Wesley Publishing Co., Inc., 1973.

48. Bigg, Donald M., "Mechanical, Thermal, and Electrical Properties of Metal Fiber-Filled Polymer Composites", *Polym. Eng. Sci.*, Vol. 19, No. 16, 1979, pp. 1188-1192.

49. Sundstrom, Donald W., and Lee, Yu-Der, "Thermal Conductivity of Polymers Filled with Particulate Solids", *J. Appl. Polym. Sci.*, Vol. 16, 1972, pp. 3159-3167.

50. Osborne, Tim, Union Carbide Corp., Specialty Products Group, "Personal Communication regarding Boron Nitride".

VITA

Keith Brown was born on August 25, 1961 to Walter and Lucie Brown of Berkeley Heights, NJ. Keith attended Berkeley Elementary School and Columbia Junior High School before graduating from Governor Livingston Regional High School in June, 1979. After working for several years as a television repairman, Keith finally entered college. He attended New Jersey Institute of Technology as a freshman and then transferred to Lehigh University. Following his junior year, Keith was employed in the summer pre-professional program of the International Business Machines Corporation in Poughkeepsie, NY. He received a Bachelor of Science Degree in Metallurgy and Materials Engineering from Lehigh University in June, 1986.

Keith received several awards and honors while at Lehigh. In 1984, he became a member of Tau Beta Pi, the national engineering honor society and ASM, the American Society for Metals. In 1985, he was an ASM national scholar and received scholarships from the Carpenter Technology Corporation and the Lehigh Valley Chapter of the ASM. In 1986, he received the Bradley Stoughton Student Award and the Handwerk Prize. Keith graduated with highest honors.

Since May of 1986, Keith has been an Associate Engineer with the International Business Machines Corporation in Poughkeepsie, NY. Keith received a fellowship from the Lehigh University Alumni Association. In January, 1987, Keith enrolled in the Department of Materials Science and Engineering at Lehigh and began his studies in Manufacturing Systems Engineering.